Proceedings World Geothermal Congress 2026
Calgary, Canada, June 8 – 11, 2026

Exploring the Relationship Between Measured Tracer Adsorption Uncertainty and Resulting Thermal Breakthrough Predictions

Eito Miyakoshi[1*], Shigemi Naganawa[1] and Elvar K. Bjarkason[1]
Graduate School of International Resource Sciences, Akita University, Japan[1]
* m6025223@s.akita-u.ac.jp

Keywords: Tracer test, reactive tracer, partition coefficient, adsorption rate, uncertainty

ABSTRACT

Understanding the potential for thermal breakthrough (both its extent and rate) is critical when planning and managing fluid reinjection in geothermal reservoirs. Thermal breakthrough occurs when cool reinjection fluids migrate to production wells, resulting in a drop in the produced fluid temperature and, consequently, a loss in energy production efficiency. Accurately predicting this phenomenon is vital for optimizing reservoir longevity and economic performance.

One promising technique for predicting thermal breakthrough behavior involves using reactive tracers (chemical solutes) that can adsorb onto reservoir rock surfaces. Under idealized conditions, the adsorption properties of these tracers can be exploited to infer properties of subsurface flow paths and estimate thermal front progression with high precision. This makes adsorptive tracer tests an appealing diagnostic tool for geothermal engineers and reservoir modelers. However, practical application of this method is complicated by the inherent uncertainties in tracer-rock interactions. These interactions can vary significantly depending on site-specific factors such as mineral composition, fluid chemistry, and temperature. This study considers tracer-rock adsorption experiments to explore the effects of tracer adsorption uncertainty on thermal breakthrough predictions.

In this study, batch adsorption experiments were first conducted to estimate adsorption parameters for lithium ions sorbing onto granite. Two granite rock samples with nominal surface areas of 30.2 cm^2 (R1) and 64.8 cm^2 (R3) were compared. The posterior mean for the estimated adsorption rate constant and partition coefficient were 1.58 1/s and 0.01 m for R1, and 1.58 1/s and 0.02 m for R3, respectively. Subsequently, numerical simulations were performed to evaluate the derived uncertainty of tracer tests under field-scale conditions and resulting temperature predictions. The results suggested that the uncertainty in temperature-decline predictions could reach approximately 32°C for R1 and 34°C for R3. These findings indicate that the uncertainty in adsorption-related parameters significantly affects the uncertainty in temperature-decline predictions.

1 INTRODUCTION

Geothermal power generation is a renewable energy source that emits a relatively low amount of carbon and enables continuous electricity production. As it operates mostly independently of weather and other natural conditions, it serves as a reliable baseload power source unlike other renewables. Moreover, geothermal fluids can be further used for applications such as greenhouse cultivation, offering additional economic benefits to local communities. These features make geothermal energy a valuable resource for the future.

However, several challenges remain for geothermal energy despite its steady baseload power supply. These include the high risks and costs of development, spatial concentration of geothermal potential that limits suitable sites and grid connectivity, and the necessity to coordinate with local stakeholders and navigate complex regulatory frameworks. Another major operational challenge in geothermal power generation is the temperature decline that occurs in both the produced fluid and the reservoir due to fluid reinjection. This issue arises from the rapid influx of reinjected cold water into production wells, which can lead to a significant and untimely drop in production temperature. Such processes ultimately lead to reduced energy extraction efficiency, shorter reservoir longevity, and higher operational costs. Therefore, timely prediction of the extent and rate of temperature decline that will be caused by ongoing and planned reinjection strategies is desirable. Reservoir engineers often look to using tracer tests to probe the connectivity of injection and production wells with the goal of understanding the potential effects of reinjection (Reimus et al., 2012; Rose et al., 2012).

This study looks at the advantages of using lithium-ion tracers as reactive tracers (Dean et al., 2015) to estimate the principal reservoir parameters determining the rate of temperature decline. Here we present results of early

batch reaction experiments aimed at quantifying the expected uncertainty of parameters governing sorption of lithium ions onto rock samples. Finally, we consider how those uncertainties extend to the interpretation of tracer injection tests that are meant to inform temperature decline predictions in the field.

2 METHODOLOGY

In this study, we conducted batch adsorption experiments using lithium ions as the sorbing tracer and granite rock samples representing the reservoir formation, followed by numerical simulations to extend the experimental results to field-scale tracer tests and to quantify the uncertainty in temperature-decline predictions. The simulation framework was developed based on the modeling approaches presented by Hawkins et al. (2018) and Bjarkason (2023).

2.1 Tracer Test

A tracer test is a diagnostic technique used to identify subsurface flow paths and flow rates, providing insights into flow dynamics and mass transport within geothermal reservoirs. However, using conventional, non-reactive tracers provides limited insights into the thermal influence of fluid reinjection on production wells and the reservoir. To address this limitation, adsorptive tracers—whose transport behavior depends on the reactive surface area of reservoir rocks—have been investigated as potential tools to reduce the uncertainty of future temperature-decline predictions. Figure 1 outlines the main elements of an adsorptive tracer test where both inert and sorbing tracers are injected into a reservoir. The tracer arrival is subsequently measured in the production well and the observed tracer response is analyzed to reveal reservoir parameters that are relevant for temperature decline prediction.

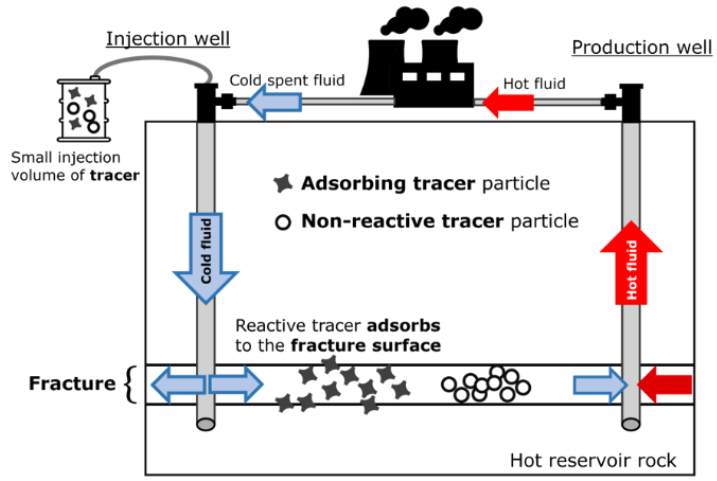


Figure 1. Schematic of a tracer test involving an inert (non-reactive) tracer and a reactive (sorbing) tracer.

2.2 Batch Adsorption Experiment

A batch adsorption experiment is a laboratory technique in which samples and reagents are mixed and allowed to react under controlled conditions for a specified duration to evaluate sorption of the reagent onto the sample material. In this study, adsorption batch tests were performed by immersing granite samples in lithium-ion solutions and periodically measuring ion concentrations in the fluid to quantify the extent of lithium adsorption onto the rock surface (Figure 2). The obtained data were used to estimate the adsorption-rate and equilibrium partition coefficient of the adsorptive tracer, which serve as fundamental inputs for constructing transport models describing sorbing tracers in geothermal reservoirs.

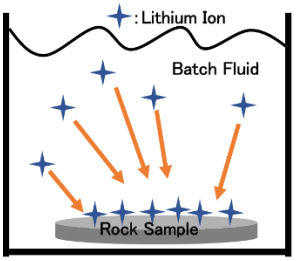


Figure 2. Schematic of a batch adsorption test.

Two granite rock samples with nominal surface areas of 30.2 cm^2 (sample R1) and 64.8 cm^2 (sample R3) were prepared (Figure 3). Each sample was immersed in 200 mL of a 10 ppm lithium-ion standard solution for approximately one month. The solution temperature was maintained at 24°C using a heat bath (Figure 3), and 1 mL of the test solution was periodically sampled and diluted with 99 mL of purified water to produce 100 mL solution samples. After the experiment, the lithium-ion concentration in each sample was measured using Microwave Plasma–Atomic Emission Spectroscopy (MP-AES). The concentration evolution for each reaction experiment was then modeled.

The physical model equations used to describe the tracer adsorption during the batch experiments are expressed as follows (Bjarkason and Hawkins, 2023).

$$\frac{\partial c}{\partial t} = -\frac{A}{V}\frac{\partial \Gamma}{\partial t} \tag{1}$$

$$\frac{\partial \Gamma}{\partial t} = k_{ads}\left(P_f c - \Gamma\right) \tag{2}$$

Equation (1) describes the temporal evolution of the tracer concentration in the liquid phase, whereas Equation (2) is the kinetic rate law for adsorption at the solid surface. Here, c denotes the tracer concentration in the fluid, Γ is the surface concentration of tracer adsorbed on the rock, A is the surface area of the rock sample, V is the total volume of the test solution, k_{ads} denotes the adsorption rate constant, P_f is the tracer partition coefficient, and t is time.

An analytical solution can be obtained to describe the temporal evolution of the tracer concentration by solving Equations (1) and (2) simultaneously (Bjarkason and Hawkins, 2023). Assuming that the fluid volume can be considered approximately constant during the experiment, the fluid concentration over time is described by

$$c(t) = C_0 \left[\frac{P_f}{P_f + \frac{V}{A}} \mathrm{e}^{-k_{ads}\left(\frac{A}{V}P_f + 1\right)t} + \frac{1}{\frac{A}{V}P_f + 1}\right] \tag{3}$$

This is a closed-form solution of a simultaneous first-order ordinary differential equation representing simultaneous mass transfer—adsorption and desorption—between the liquid and solid phases. The prefactor C_0 is the initial batch fluid concentration.

The reaction rate (k_{ads}) and partition coefficient (P_f) can be estimated by fitting Equation (3) to the measured concentrations from the batch experiment. Here, we used the Randomized Maximum Likelihood (RML) method (Oliver et al., 1996; Oliver, 2017) to quantify the uncertainty of those reaction parameters given the recorded concentration data.

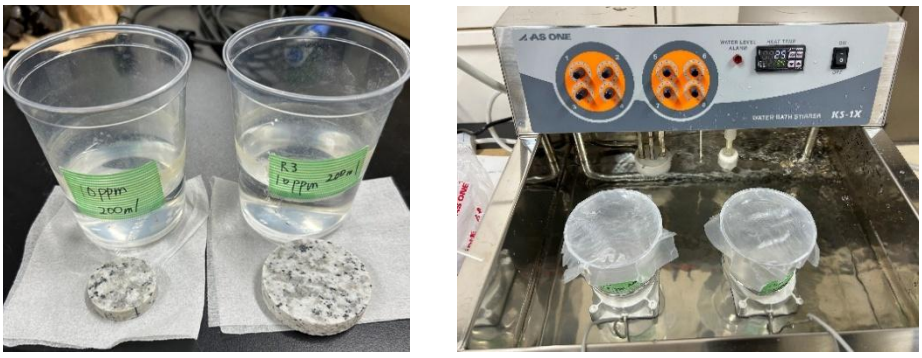


Figure 3. Photos of the setup used for the batch adsorption experiments. (Left) Granite rock samples R1 and R3. (Right) Heat bath.

2.3 Simulation of Field Tracer Injection Test

Using the posterior mean values of k_{ads} and P_f estimated by applying Equation (3) and the RML method to analyze the data from the batch adsorption experiments, field-scale tracer simulations were conducted. The simple tracer transport models considered here describe the transport of non-reactive and adsorbable tracers along a rectangular fracture. The tracer transport equations are shown in Equations (4) to (6) (Bjarkason, 2023).

$$\bar{c_p}(s) = F\frac{M}{Q_P}\exp\left[\frac{Pe}{2}\left(1-\sqrt{1+4\frac{k_f A+sV)}{qPe}}\right)\right] \quad (4)$$

$$k_f = \frac{sP_f k_{ads}}{k_{ads}+s} \quad (5)$$

$$c_p(t) = FM\frac{q}{Q_P}\sqrt{\frac{PeV}{4\pi(qt)^3}}\exp\left[-\frac{Pe(V-qt)^2}{4Vqt}\right] \quad (6)$$

These equations give the tracer concentration at the production well (c_p). Equations (4) and (5) describe the transport of a reactive tracer. Equation (4) represents the analytical solution of the tracer concentration in the Laplace domain, while Equation (5) is the term in Equation (4) expressing the adsorption reaction in the Laplace domain. Equation (6) provides the time-domain solution for the case of an inert tracer. Here, F denotes the tracer recovery fraction, Pe is the Peclet number, M is the tracer mass injected, Q_P is the volumetric production rate, q is the volumetric flow rate within the fracture, V is the fracture volume, and s is the Laplace variable.

Apart from the tracer reaction parameters gathered from the batch experiments, the tracer field response was simulated using the model parameter values listed in Table 1. Two scenarios of tracer field data are plotted in Figure 6.

Table 1. Reference simulation parameters for the field tracer test and the temperature-decline response.

Parameters		Values Used
Q_P, Q_I	Production and injection rate	0.05 [m^3/s]
F	Tracer recovery fraction	40 [%]
q	Flow rate in fracture	0.02 [m^3/s]
M_{inert}	Mass injected of inert tracer	50 [kg]
$M_{reactive}$	Mass injected of adsorptive tracer	50 [kg]
V	Fracture volume	2.0×10^4 [m^3]
A	Fracture surface area	1.0×10^6 [m^2]
Pe	Peclet number	50
k_{ads}	Adsorption rate	1.58 [1/s]
P_f	Partition coefficient	0.01 (R1), 0.02 (R3) [m]
T_0	Initial reservoir temperature	200 [°C]
T_i	Temperature of reinjection fluid	80 [°C]
K_R	Thermal conductivity of rock	7.6 [W / m·K]
ρ_R	Rock density	2500 [kg /m^3]
C_R	Specific heat capacity of rock	930 [J / kg·K]
ρ_w	Density of fluid	995 [kg / m^3]
C_w	Specific heat capacity of fluid	4190 [J / kg·K]

2.4 Estimation of Fracture Surface Area from Tracer Response

The fracture surface area is the main parameter controlling the rate of temperature decline. Notably, the goal of the adsorptive tracer test is to constrain/estimate the fracture surface area. Here we estimated the surface area by matching the tracer return profiles observed in the field with the analytical tracer transport Equation (4). Like in the case of the batch experiment, we used the RML method to quantify the uncertainty of the estimated surface area.

In general, the unknown variables in Equation (4) are the fracture volume, the tracer recovery fraction, the Peclet number, the flow rate, the fracture surface area, the tracer partition coefficient, and the tracer reaction rate. The injected mass M is usually prescribed by the field team and is commonly assumed to be known. The inert tracer response can be used to estimate the first three parameters. Therefore, to focus attention on the effect of the uncertain reaction parameters pertaining to the sorbing tracer, we assume that the only unknowns are the fracture surface area, the partition coefficient, and the reaction rate.

When analyzing field responses, we assumed that the prior uncertainties in k_{ads} and P_f are appropriately quantified based on the batch experiment results. Under this assumption, we again employed the RML method to estimate surface area uncertainties from tracer field data.

2.5 Simulation of Temperature Drop Prediction

Using the fracture surface area estimation results obtained from the tracer test, the uncertainty of temperature-decline predictions can be evaluated. The model equations used for the temperature decline predictions are presented below.

$$(\rho C)_w \left(\frac{\partial T_f}{\partial t} + v\frac{\partial T_f}{\partial x}\right) = K_R \frac{A}{V}\frac{\partial T_R}{\partial y}\bigg|_{y=\frac{V}{A}} \quad , \quad |y| < \frac{V}{A} \tag{7}$$

$$(\rho C)_R \frac{\partial T_R}{\partial t} = K_R \frac{\partial^2 T_R}{\partial y^2} \ , \quad |y| \geq \frac{V}{A} \tag{8}$$

Equation (7) represents the energy balance of the fluid in the fracture and heat exchange with the surrounding rock through heat conduction. Equation (8) represents heat conduction in the rock surrounding the fracture. Equation (8) is valid only in the solid region outside the fracture and does not include advective transport of fluids. Here, T_f is the fluid temperature in the fracture, T_R is the rock temperature, K_R is the rock thermal conductivity, C denotes specific heat capacity, and ρ denotes density. The subscript R indicates properties of the rock formation, and the subscript w indicates the fluid properties. The variable v is the mean flow velocity, x is the distance along the flow direction, and y is the position perpendicular to the fracture surface. The fracture aperture is given by $2V/A$.

$$T_f(t, L) = T_0 - (T_0 - T_i)\mathrm{erfc}\left[\frac{\eta A}{2q}\left(t - \frac{V}{q}\right)^{-\frac{1}{2}}\right] H\left(t - \frac{V}{q}\right) \tag{9}$$

$$\eta = \frac{\sqrt{K_R(\rho C)_R}}{(\rho C)_w} \tag{10}$$

$$T_p(t) = T_0 - \frac{FQ_I}{Q_P}\Big(T_0 - T_f(t, L)\Big) \tag{11}$$

Equation (9) provides an analytical solution for fluid temperature at the fracture outlet as the fluid enters the production well. Equation (10) represents the thermal parameters, and Equation (11) represents the temperature observed at the production well. Here, T_0 is the initial temperature of the geothermal reservoir, T_i is the temperature of the reinjected fluid, $T_f(t, L)$ is the fluid temperature at the fracture outlet, Q_I and Q_P are the injection and production flow rates, respectively, and H is the Heaviside step function.

3 RESULTS

3.1 Batch Adsorption Test Results

The measured data from the first hour of the batch adsorption experiments is shown in Figure 4. Although the initial batch fluid concentration for the lithium tracer was designed to be 10 ppm, both experiments R1 and R3 had a higher measured initial concentration. The measured initial concentrations were approximately 14 ppm

and 12 ppm for the R1 and R3 rock samples, respectively. As the experiment progressed, the concentrations levelled off at around 11 ppm and 9 ppm for the R1 and R3 rock samples, respectively. Those values are mostly consistent with the prescribed initial concentration of 10 ppm. Therefore, the high initial concentration measurements may be considered as outliers, and the lithium-ion tracer may likely not have adsorbed to the rock in a perceivable way. Nevertheless, to demonstrate the uncertainty quantification workflow and the effect of the uncertainty of the batch experiments, we decided to analyze the batch data as though the initial concentration could be considered reliable.

Fitted model bounds are shown in Figure 4 for both experiments. The model uncertainties are indicated by the estimated 95% credibility intervals (CIs). The posterior distributions of the estimated adsorption rate constant (k_{ads}) and partition coefficient (P_f) are shown in Figure 5.

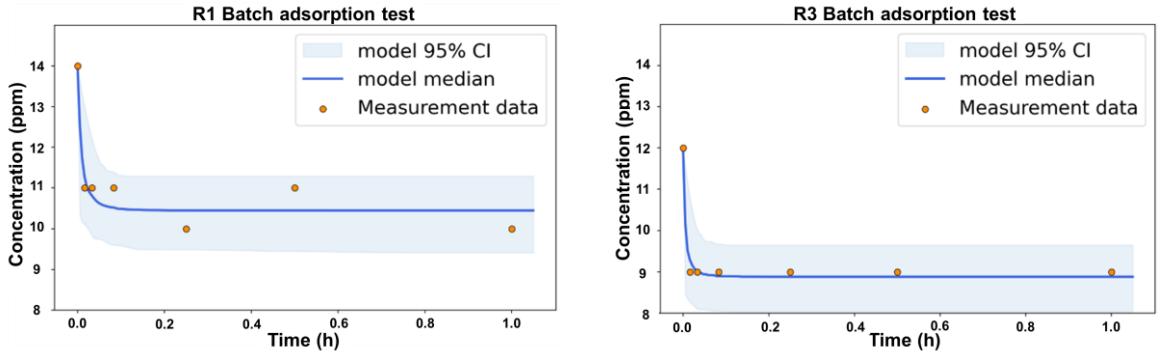


Figure 4. Batch adsorption test results and modeled reaction profiles. (Left) Sample R1. (Right) Sample R3.

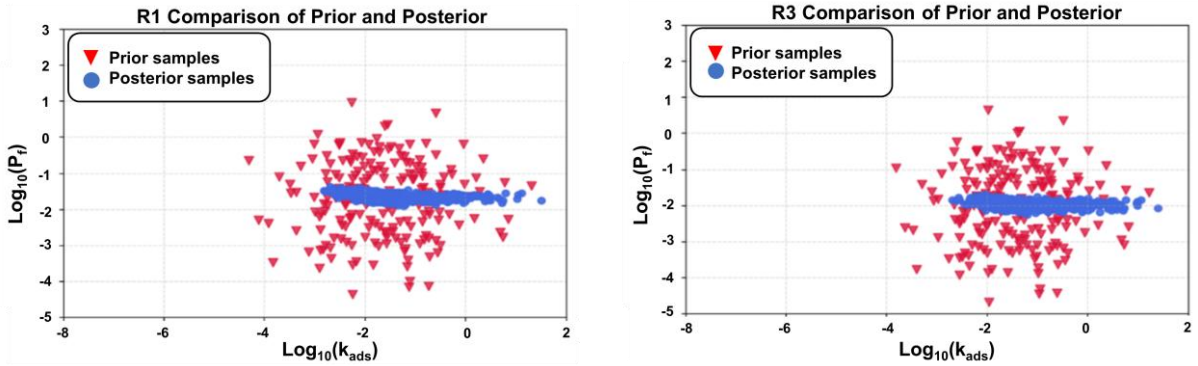


Figure 5. Estimated uncertainty of adsorption parameters k_{ads} and P_f. (Left) sample R1. (Right) sample R3.

The estimated posterior means obtained using the RML method for the adsorption rate constant (k_{ads}) and partition coefficient (P_f) were 1.58 [1/s] and 0.01 [m] for the 30.2 cm^2 sample (R1), and 1.58 [1/s] and 0.02 [m] for the 64.8 cm^2 sample (R3), respectively.

3.2 Results of Simulated Tracer Tests

The results of the field-scale tracer simulations are shown in Figure 6. The inert tracer arrives at the same time for both cases because the fracture geometry and other parameters influencing the inert tracer transport were assumed the same for cases R1 and R3. However, the reactive tracer arrives later for simulation case R3 because of the higher partition coefficient. Additionally, the simulated data includes random observation noise. The standard deviation of the noise was set to 5% of the maximum tracer concentration. As a result, the inert tracer data is slightly different for the two cases. Nevertheless, the differences in the inert tracer data did not influence the uncertainty quantification reported here because the simplified analysis only considered the reactive tracer data as described previously.

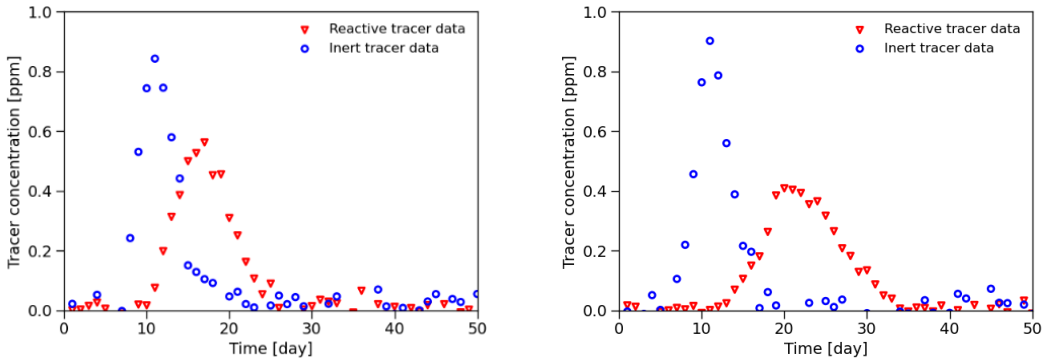


Figure 6. Tracer return curves for tracer field tests. (Left) Sample R1. (Right) Sample R3.

In the synthetic tracer simulations, a reference fracture surface area was prescribed to generate the tracer return responses shown in Figure 6. However, during the inversion step, the fracture surface area was treated as an unknown parameter and estimated together with the adsorption rate constant (k_{ads}) and the partition coefficient (P_f) using the RML method. Therefore, although a single reference value was used to generate the synthetic data, the posterior analysis resulted in a distribution of plausible surface area values conditioned on the tracer observations.

3.3 Uncertainty Assessment of Temperature Decline Prediction

Based on the results presented in Sections 3.1 and 3.2, the simulation of temperature-decline prediction uncertainty in the geothermal reservoir yielded the results shown in Figure 7. From these results, the uncertainty in temperature-decline predictions was found to reach a maximum of about 32°C for R1 and 34°C for R3 (based on 95% CIs). This is about 70% of the maximum expected temperature change $F(T_0 - T_i)$ = 48°C. Such uncertainty levels would limit detailed tuning of reinjection strategies and economic decision-making. However, these results are based on questionable batch adsorption data and further experiments are needed to better understand the uncertainty of lithium adsorption.

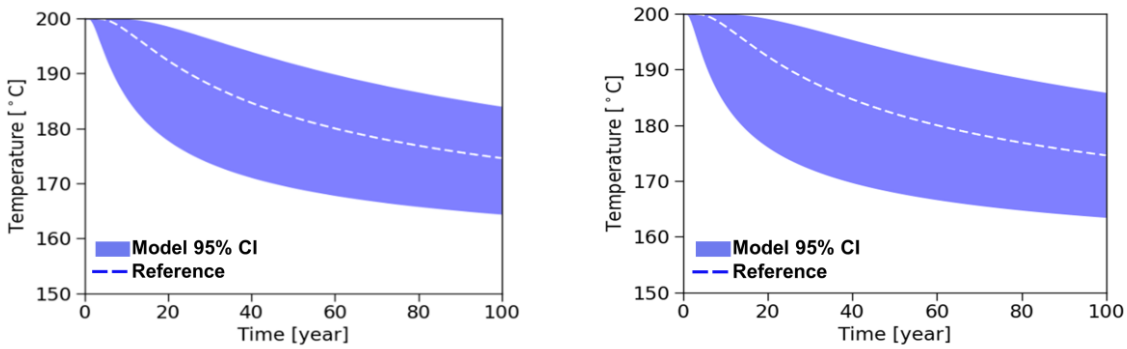


Figure 7. Uncertainty of temperature decline predictions. (Left) Sample R1. (Right) Sample R3.

4 CONCLUSION

When considering lithium-ion tracers for predicting temperature decline in geothermal reservoirs, it was found that the predictions involved a degree of uncertainty, primarily influenced by uncertainties in adsorption-related parameters. Among the governing factors, the fracture surface area (A), the adsorption rate constant (k_{ads}), and the partition coefficient (P_f) were considered as dominant parameters controlling the predictive variability. For this pilot demonstration, uncertainties from the tracer batch adsorption experiment translated to temperature prediction errors up to approximately 30°C. Future work will include testing a larger number of rock samples to evaluate adsorption characteristics under various conditions. In addition, we plan to investigate the use of cesium ions as an alternative to lithium ions, modify experimental parameters such as temperature, duration, and rock surface area, and reassess the parameters used in the field-scale tracer and temperature-decline simulations.

Acknowledgements

This study was supported by JSPS KAKENHI Grant Number JP24K17640. Appreciation is also extended to Professor Tadao Imai of the Rock Engineering Laboratory at Akita University for kindly providing the rock samples used in the experiments.

REFERENCES

Bjarkason, E.K.: How precise can thermal breakthrough predictions be that are derived from adsorptive tracer tests?, *Proceedings, 48th Workshop on Geothermal Reservoir Engineering*, Stanford University, Stanford, CA, (2023).

Bjarkason, E.K., and Hawkins, A.J.: Preliminary evaluation of cesium tracer adsorption for geothermal applications: Implications for temperature decline predictions, *Proceedings, International Symposium on Earth Science and Technology*, Kyushu University, Fukuoka, Japan, (2023).

Dean, C., Reimus, P., Oates, J., Rose, P., Newell, D., and Petty, S.: Laboratory experiments to characterize cation-exchanging tracer behavior for fracture surface area estimation at Newberry Crater, OR, *Geothermics*, 53, 213–224, (2015).

Hawkins, A.J., Becker, M.W., and Tester, J.W.: Inert and adsorptive tracer tests for field measurement of flow-wetted surface area, *Water Resources Research*, 54 (8), 5341–5358, (2018).

Oliver, D.S.: Metropolized randomized maximum likelihood for improved sampling from multimodal distributions, *SIAM/ASA Journal on Uncertainty Quantification*, 5(1), 259–277, (2017).

Oliver, D.S., He, N., and Reynolds, A.C.: Conditioning permeability fields to pressure data, *Proceedings, 5th European Conference on the Mathematics of Oil Recovery*, Leoben, Austria, 259–270, (1996).

Reimus, P., Williams, M., Vermeul, V., Rose, P., Leecaster, K., Ayling, B., Sanjuan, R., Ames, M., Dean, C., and Benoit, D.: Use of tracers to interrogate fracture surface area in single-well tracer tests in EGS systems, *Proceedings, 37th Workshop on Geothermal Reservoir Engineering*, Stanford University, Stanford, CA, (2012).

Rose, P., Leecaster, K., Clausen, S., Sanjuan, R., Ames, M., Reimus, P., Williams, M., Vermeul, V., and Benoit, D.: A tracer test at the Soda Lake, Nevada geothermal field using a sorbing tracer, *Proceedings, 37th Workshop on Geothermal Reservoir Engineering*, Stanford University, Stanford, CA, (2012).